EUROPEAN ORGANIZATION FOR NUCLEAR RESEARCH
Laboratory for Particle Physics

THIN CRYOGENIC X-RAY WINDOWS

T.O. Niinikoski[1], B. Bellanger[1], M. Davenport[1], N. Elias[1], S. Aune[2], J. Franz[3]

We describe the construction and tests of cryogenic X-ray windows of 47 mm diameter made of 15 ìm thick polypropylene foil glued on a UHV flange and supported with a strongback mesh machined by electro-erosion. These hermetic windows of the solar axion telescope of the CAST experiment at CERN withstand the static and dynamic pressures of the buffer gas that are normally below 130 mbar, but may reach 1.2 bar when the magnet quenches. They were tested at 60 K up to 3.5 bar static pressure without permanent deformation.

1 CERN, Geneva, Switzerland
2 CEA-Saclay, DSM/IFRU, Gif-sur-Yvette, France
3 Albert-Ludwigs-Universität, Freiburg, Germany

Thin cryogenic X-ray windows

Niinikoski T.O., Bellanger B., Davenport M., Elias N., Aune S.*, Franz J. **

CERN, 1211 Geneva 23, Switzerland
* CEA-Saclay, DSM/IFRU, F-91191 Gif-sur-Yvette , France
**Albert-Ludwigs-Universität, D-79104 Freiburg, Germany

We describe the construction and tests of cryogenic X-ray windows of 47 mm diameter made of 15 µm thick polypropylene foil glued on a UHV flange and supported with a strongback mesh machined by electro-erosion. These hermetic windows of the solar axion telescope of the CAST experiment at CERN withstand the static and dynamic pressures of the buffer gas that are normally below 130 mbar, but may reach 1.2 bar when the magnet quenches. They were tested at 60 K up to 3.5 bar static pressure without permanent deformation.

INTRODUCTION

The telescope of the CAST experiment [1] at CERN is designed to search for the hypothetical axions originating from X-rays converted by the Primakoff mechanism in the strong magnetic field of the solar core. The detection of axions is based on conversion back into X-rays in the strong transverse field of a decommissioned prototype dipole magnet of the Large Hadron Collider. In order to extend the axion mass reach of the experiment above 0.02 eV, the cold bores of the dipole need to be filled with buffer gas that maintains, by adjusting the index of refraction, the phase coherence between the axion and the photon during their 9 m long travel through the field of 9 T. The density of the gas must be accurately controlled during data runs, because the coherence can be maintained only in a relatively narrow range of axion rest masses. The two cold bore tubes therefore need to be closed with four cryogenic windows that are sufficiently transparent to X-rays in the range of 2 keV to 8 keV. This requires the use of very thin low-Z material, such as Be or a plastic. Additional requirements for these windows are resistance to static and dynamic pressures during normal operation and when the magnet quenches, low permeability to helium, absence of pinholes, and transparency to visible light. The transparency enables simple alignment, checking of contaminants on the windows, and experiments with low-energy axions of solar or other origin.

As the cold bore tubes are operated at 1.8 K temperature, only ^{4}He and ^{3}He are qualified as buffer gas. Their saturation pressures at 1.8 K temperature are 16.405 mbar and 135.58 mbar, which limit the ranges of axion mass reach to about 0.3 eV and 1.2 eV, respectively. We describe here the construction and tests of the windows of 47 mm diameter that confine the buffer gas into the cold region of the bore tubes.

The results of CAST [2] without buffer gas have been published, and those with [4]He buffer gas, confined by the above windows, are forthcoming [3]. The run with [3]He buffer gas is underway. We refer to papers [1 — 3] for more detailed information on the experiment.

WINDOW DESIGN AND FABRICATION

The windows, shown in Figure 1, consist of a cylindrical part made of AISI 316LN stainless steel with CF63 UHV flange knives at both ends, foreseen to be assembled between two fixed CF63 flanges of the cold bore tubes. On one side a strongback is machined by electro-erosion. This consists of 5.2 mm square mesh, with 0.3 mm wide and 5 mm deep struts that serve as supports for the window film.

The 15 µm thick polypropylene (PP) or 23 µm thick polyethylene terephthalate (PET) film is glued onto the strongback struts and surrounding flange using Araldite 2018 epoxy, and a stainless steel top ring is glued both to the polypropylene film and to the flange to give extra resistance against peeling and to provide mechanical protection. The details of the glued joint are shown in Figure 1.
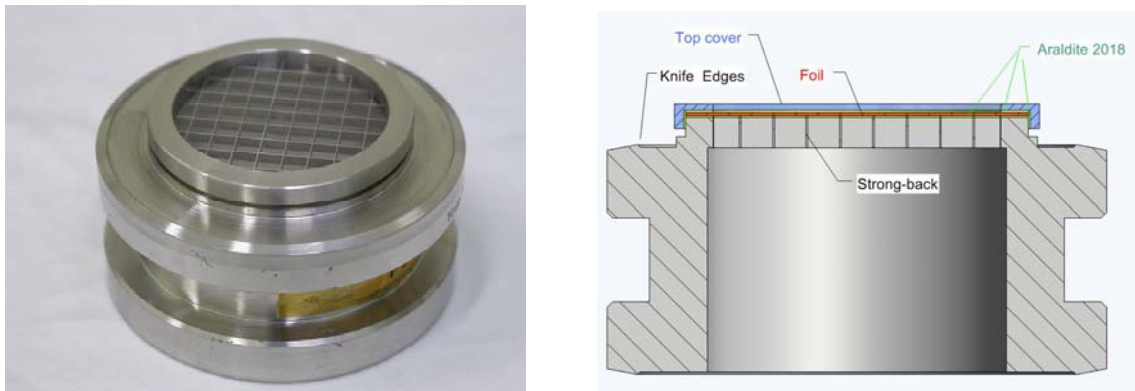

Figure 1 Window mounted on CF63 flange: photograph (left); cross section (right).

The PP film is manufactured by the Blown Film Extrusion (BFE) method, in which the plastic melt is extruded through an annular slit die to form a thin walled tube. Air is introduced via a hole in the centre of the die to blow up the diameter of the tube like a balloon. The drawdown of thickness between the melt and the cooled film occurs in transverse and longitudinal directions and is controlled by changing the volume of air inside the bubble and by altering the haul off speed. This biaxial stretching gives the film a better balance of properties than cast or extruded film that is drawn down along the extrusion direction only.

The electro-erosion of the strongback was done with 0.25 mm diameter wire to a precision of $\pm$ 0.01 mm. The surfaces were cleaned by 4 h immersion in water solution of 50% HNO_3 and 3% HF, which produced a rounding of about 5 µm of the sharp edges. The subsequent 2 min electro-polishing produced a final rounding of ~ 30 µm and left 240 µm wide flat surfaces to glue the film onto the 300 µm wide struts. The Araldite 2018 epoxy glue was printed on the strongback ring and struts with silkscreen. The film, attached to a frame, was stretched lightly with a pneumatically controlled force when pressing the film onto the strongback. The polish of the top surfaces was reduced by light grinding before gluing.

The windows were submitted to 1 bar pressure difference before and during their cooldown when leak testing. This gives the film a round dome shape that freezes in when the film loses its plasticity upon cooldown. The dome shape is theoretically stronger than the planar shape obtained when cooling the film

without pressure. Immediately after warm-up the film showed wrinkles that were interpreted as anisotropy in the plastic behaviour during the initial cooldown. The mechanical testing, to be discussed below, confirmed this hypothesis.

CHOICE AND CHARACTERISTICS OF THE WINDOW MATERIAL

Figure 2 shows the theoretical transmission coefficients of X-rays through different thicknesses of PP $(C_2H_6)_n$ and PET $(C_{10}H_8O_4)_n$ films. These are strong low-Z materials that can be used in windows. As shown by the figure, however, the 4 oxygen atoms in the PET unit cell, together with its higher density, favour PP over PET with regard to X-ray transmission. Biaxially oriented PET film has at room temperature a high Young's modulus $E = 4$ GPa and ultimate tensile strength $R_m = (55-75)$ MPa, while PP films may have E varying from 1 GPa to 3 GPa, and $R_m = (20-40)$ MPa. The most important parameter against rupture, however, is the elongation at rupture, which is 50% to 150% for PET film, and can vary from a few % up to 600% for PP. The mechanical testing of the film at the operating temperature around 60 K is therefore important in order to understand and predict the behaviour of the window at high pressures.
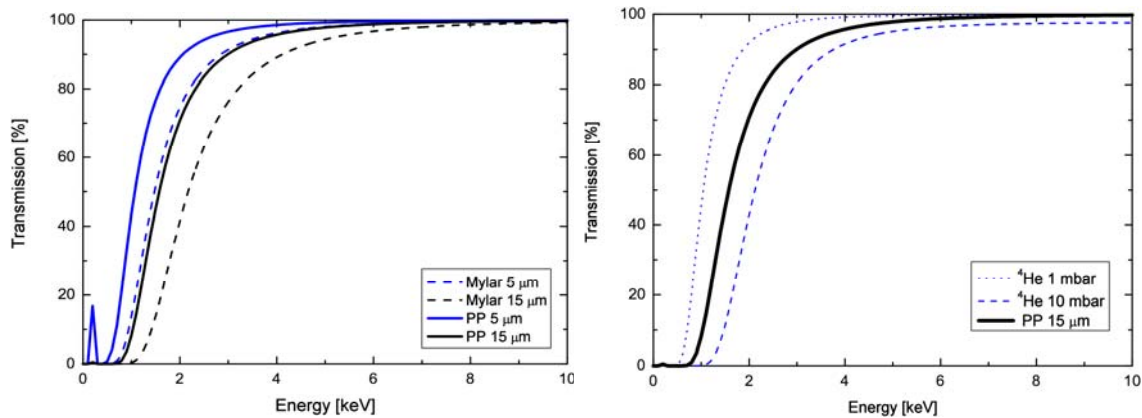

Figure 2 Theoretical X-ray transmission through foils of PP and PET (M for Mylar) (left); through 15 µm PP compared with 5 m of helium at 1 mbar and 10 mbar pressures at 1.8 K (right).

Basing on the X-ray transparency and on the helium leak performance, we have selected the 15 µm thick PP film as material for the windows to be used in the solar axion telescope of CAST.

Helium and other gases permeate through uncoated plastics by diffusion that slows down quickly when cooling to cryogenic temperatures. The diffusion is thermally activated and yields the temperature dependence of the flow rate of the gas $p\dot{V}/A = bD_0 e^{-(E_a/kT)}\Delta p/h$ [4], where p is the upstream pressure at which the volume flow rate $\dot{V}$ is measured (at standard temperature), A is the surface area of the film, b is the solubility of the gas in the plastic, D_0 is the diffusion constant of the molecules of the gas in the material, E_a is the activation energy for diffusion, and h is the thickness of the film.

Figure 3 shows the leak rate of helium through the window during the cooldown with about 1 bar helium pressure. The straight lines show the fit of the above equation to this data. The deviation from the predicted exponential behaviour is likely to be due to degassing and to the difficulty in determining the window film temperature, which may deviate from that of the UHV flange shown in Figure 2.
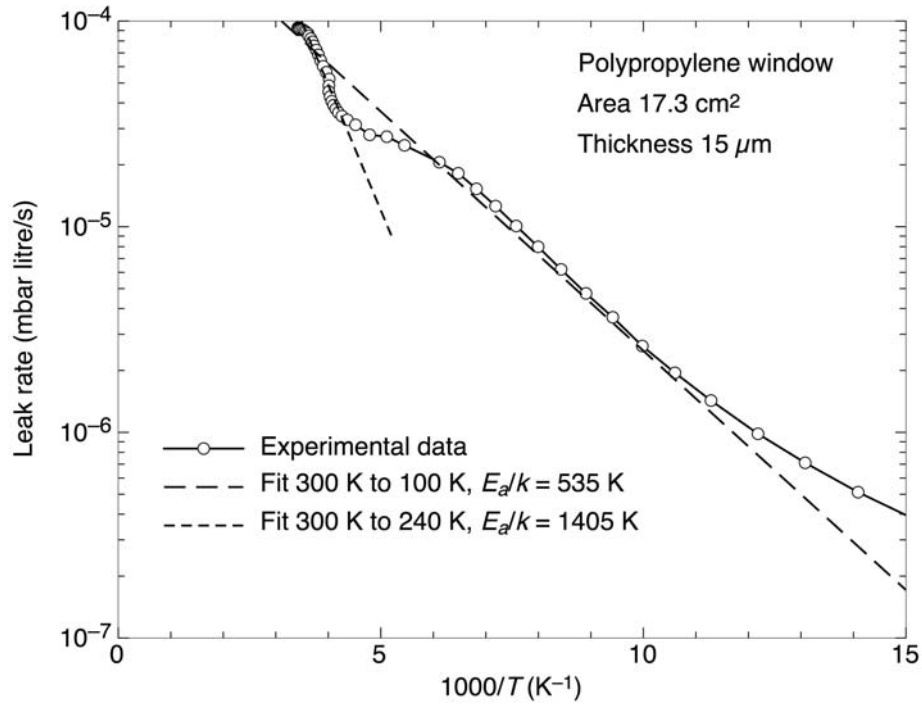
Figure 3 Measured leak of helium (round points), and fits of the data to the diffusion model (straight lines).

The fit yields $E_a/k = 535$ K and $bD_0 = 4.6 \cdot 10^{-8}$ mbar·litre/(bar·cm^2/cm). The diffusion rate at room temperature, scaled to $A = 1$ cm^2 and $h = 1$ cm, is $7.4 \cdot 10^{-9}$ mbar·litre/s, which is close to that for neoprene, $9 \cdot 10^{-9}$ mbar·litre/s. However, neoprene has a very much steeper temperature dependence, with $E_a = 6900$ K, determined from data above room temperature. Our data on PP above also suggests steeper temperature dependence near room temperature with $E_a/k = 1405$ K, which is close to the activation energy of the diffusion of helium in fused silica, $E_a/k = 1950$ K.

Among the 11 windows tested 8 showed behaviour identical to that plotted in Figure 3. Three windows had a few orders of magnitude larger leak rate already at room temperature. The leak increased upon cooling, which suggests the presence of pinholes or cracks in the film. The good windows were also cooled below the lambda point in order to verify the absence of even the smallest pinholes or cracks.

All windows were successfully tested also for rapid pressurization from vacuum to 1.5 bar. This simulates the quench of the dipole magnet, during which the mean temperature increases by a factor of 20 in about 120 s inside the cold bore tubes. The maximum quench pressure is 1.2 bar, however, because the helium is allowed to expand into a volume of 500 litres when the quench trigger signal is received.

Moreover, the integrity of one of the windows was successfully tested at 60 K up to 3.5 bar pressure during the measurement of the mechanical characteristics of the strongback, as will be described below.

Tensile tests of foil samples at 77 K revealed a substantial difference between the longitudinal and transverse properties of the film, as shown by Table 1.

Table 1 Mechanical characteristics of 15 µm PP film measured at 77 K temperature

Direction of stress	E (GPa)	Yield tensile strength (MPa)	Ultimate tensile strength (MPa)	Elongation at break (%)
Longitudinal	8.3	140	225	23.6
Transverse	13.3	240	380	10.0

Table 2 Simulated stress of the15 µm PP film at 77 K temperature

p (bar)	s_{max} (von Misès) (MPa)	d_{max} (mm)	Safety coefficient R_m/s_{max}
1.2	145	0.24	1.55
1.5	147	0.26	1.53
2.7	155	0.32	1.45
3.5	174	0.35	1.30

Due to this anisotropy, under biaxial stress produced by applied pressure, the foil will yield first in areas of large longitudinal stress. This relaxes the longitudinal stress in areas of large yield, and increases the stress in transverse direction. Therefore, the stress/strain curve in the longitudinal direction was chosen for the isotropic mechanical behaviour introduced in our ANSYS model, which is deliberately pessimistic. A square of the film limited by the struts was modelled with shell elements to 8 nodes and 6 degrees of freedom by node, in order to correctly account for the development of the dome shape of the film under pressure. The mesh features 40 x 40 x 1 elements.

The numerical results of Table 2 show that with only 1.2 bar pressure, the 15 µm polypropylene film is solicited in the plastic domain, because R_e = 140 MPa. Moreover, the tensile tests show in the longitudinal direction, although the ultimate strength is weak (R_m = 225 MPa), that the polypropylene film could undergo an important strain (elongation at break is 23 %).

MODELING AND TESTS OF THE STRONGBACK

The strongback has two perpendicular symmetry planes, which permit to reduce the finite element model to one quarter limited by the planes of symmetry. The boundary conditions feature no degrees of freedom of the nodes on the outer cylinder where the struts are fixed on the flange, and no transverse displacement of the nodes on the symmetry planes. Figure 4 represents the field of the equivalent stress of von Misès at 1.5 bar pressure distributed as a uniform load per unit length of the struts. The maximal stress for this pressure is equal to 148 MPa, located at the intersections with the massive part of the flange.
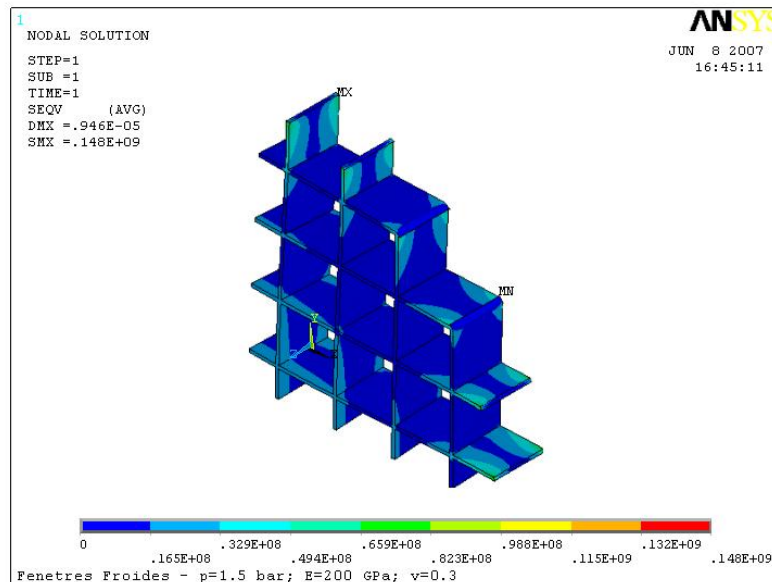
Figure 4 ANSYS simulation of the strongback at 60 K temperature and 1.5 bar pressure.

As we did not find the values for 316 LN at 60 K, we shall apply those of AISI 304 for the yield and ultimate tensile strengths, in order to obtain the safety factors of our strongback. Basing on the yield tensile strength of 450 MPa, the safety coefficient for permanent deformation of the struts is 1.3 at 3.5 bar pressure, and the ultimate pressure before plastic deformation is 4.5 bar. The safety factor against rupture of the strongback is 4.2 at 3.5 bar pressure. The rupture or peeling of the window film may occur earlier. The safety factor against buckling of the strongback struts is 26.5 at 3.5 bar pressure.

While our maximum pressure is expected to be 1.2 bar when the quench signal opens the cryogenic valve at one end of the magnet, and/or the check valve opens at the other end, CAST have based the safety factors on conditions worse than the 2.7 bar pressure resulting when no safety valve opens during a quench at full helium load of the cold bore tubes.

One of the windows was submitted to 11 cycles from vacuum to pressures varying from 1.5 bar to 3.5 bar, at 300 K, 120 K, 60 K and 6 K temperatures. The displacement of the central square of the mesh was measured by a probe connected to a linear displacement sensor. The Young's modulus E of the AISI 316 LN stainless steel was adjusted to 210 GPa to make the displacement in the simulated model coincide with the value measured at 60 K. The displacements at different temperatures then yielded the Young moduli 215 GPa at 6 K, 202 GPa at 120 K and 193 GPa at 300 K. The Poisson's ratio $v = 0.272$ was used at all temperatures. These values are quite similar to those for AISI 304, which has $E = 200$ GPa at 60 K.

CONCLUSIONS AND ACKNOWLEDGMENTS

We have shown that 15 µm thick polypropylene film, fabricated by the BFE method, is an excellent low-Z material for low-energy X-ray windows. The film can be glued on a strongback support, and it features few pinholes and other defects. Mechanical characterization at 77 K, combined with ANSYS shell modelling, suggests that the film, glued on the 5 mm x 5 mm strongback strut mesh, can withstand pressures well in excess of 3.5 bar, the highest value in our tests. At this value the strongback remains in the elastic domain. The window has low diffusion rate of helium at cryogenic temperatures.

This work was carried out mainly in the CERN Central Cryogenic Laboratory (Cryolab), where we are grateful for the technical support of L. Dufay-Chanat, S. Prunet and G. Ratcliffe. The technical support of CEA Saclay is acknowledged in the initial development of the gluing techniques. The final series of the windows was prepared, tested and glued at CERN, where the support of D. Fraissard and J.-F. Ecarnot is greatly appreciated. We would also like to thank the workshop of U. Freiburg for machining many of the flanges.

REFERENCES

1. CAST Collaboration, C.E. Aalseth *et al.*, SPSC/P312 (9 August 1999).
2. CAST Collaboration, K. Zioutas *et al.*, Phys. Rev. Lett. 94 (2005) 121301 [arXiv:hep-ex/0411033].
3. CAST Collaboration, K. Zioutas *et al.*, Status Report of the CAST experiment CERN-SPSC-2007-013.
4. A. Roth, *Vacuum Technology*, North Holland Publishing, Amsterdam 1982, pp. 163–165.